



Ice Trial with RV Lance in March 2014, Ice Route Optimisation Project

Photograph by Stefan Hendricks,AWI

IN THIS ISSUE:

- Ice Routing Optimization IRO-2 Validation Trial
- Viscous Flow Supported Skeg Optimisation for an Articulated Tug-Barge Unit
- Towards Ships with Low Wave Drag
- Measurements of Wave Added Resistance in Oblique Seas
- Reliable Prediction of Ship Motions in Seaways for Complex Hullforms
- TARGETS achieved
- Sea Trial Procedure Updates for EEDI Verification
- Emission Reduction During Port Manoeuvring
- Pre-Swirl Stators for Deltamarin: Efficiency in Propulsion Meets Efficient Cooperation
- Member of Staff
- Cavitation Documentation and HYKAT Control Goes Android



SMM 2014
9th–12th September

Dear reader,

Meeting the ambitions to make shipping a more sustainable industry will require industry to mobilise new technologies, new solutions and new operational functions. Key issues will be safe operation, advanced ship and propeller designs, future materials and paints.

The Arctic is changing and therefore opportunities are opening up for the offshore, gas and shipping industry as a whole. Up to now the industries are far from being ready to deal with all the challenges and this means needs for detailed research. Ship design is the first in a ship's life, it is the key issue to optimize performance and to develop safer, greener and smarter vessels. Energy efficiency will without any doubt continue to be the main driver for the evolution of ship designs. Additionally the installation of numerous offshore wind farms creates an additional demand for specialized vessels.

This needs on one side more testing, but as calculations by CFD-methods become more advanced, ship designers will have access to more precise data concerning ship's

behavior for example in different seaways and enabling them to check their designs in different operating conditions and variable environments in an early design stage.

In these difficult times for the maritime industry networking, knowledge transfer and marketing are of fundamental importance for companies trying to hold their position in the face of strong competition.

When it comes to improve ship efficiency, propellers matter as much as the engines that power them. How much further can propeller technology go especially when it is combined with other energy saving devices such as pods, bulbs, fins, Mewis ducts, vane wheels, asymmetric sterns?

We would very much appreciate to discuss with you your innovations, your new ideas and your inventions in these fields.

You are always welcome here in Hamburg and we will try to assist you with all our experience to make your new product a success.

Juergen Friesch - Managing Director

Supported by:



on the basis of a decision
by the German Bundestag

Ice Routing Optimization IRO-2 Validation Trial



by P. Jochmann¹⁾, N. Reimer¹⁾,
L. Kaleschke²⁾, G. Müller²⁾, B. Fock²⁾,
F. Kauker³⁾, J. Asseng⁴⁾, J. Holfort⁵⁾

Increasing shipping activities in Polar regions and the requirement of safe and efficient navigation in Arctic waters motivated a group of German scientists and engineers, led by HSVA, to establish the three years lasting research project IRO-2 and request funding from the German Ministry of Economics and Energy. The objective of IRO-2 is the development of a software tool predicting an optimized route between Arctic locations using sea ice thickness and concentration forecast based on a coupled Atmosphere-Sea Ice-Ocean-Model. The predicted route together with the forecasted ice information can be displayed in different layers on an ECDIS-System. An overview about the Ice routing Service is shown in Fig. 1. During the first 2 years the different software modules were developed and interlinked while in the third year a full scale trial was scheduled for March 2014 to validate the system. On Thursday, March 13th a group of scientists and engineers of the IRO-2 consortium led by Dr. Gerd Müller from the University of Hamburg, IfM, arrived in Longyearbyen to board the



Fig. 2: R/V Lance at Longyearbyen Harbor

Norwegian Research Vessel Lance. Lance was chartered by the University of Hamburg for a validation trial to check and assess the “Ice Routing Optimization System”. The trial area was bounded in the north by the island KVITØYA and in the east by the 40th meridian.

For this trial R/V Lance was equipped with various kind of sensors to determine among other items

- Sea-water temperature, salinity and density, CTD
- Sea ice thickness and concentration, EM-31 (Fig. 3)
- Vessel movement (6 DoF), multi antenna GNSS.

In addition the University of Hamburg deployed drift buoys to investigate the ice drift speed and direction. NPI operated a helicopter with an EM-Bird to measure ice and snow thickness in the vicinity of the Lance

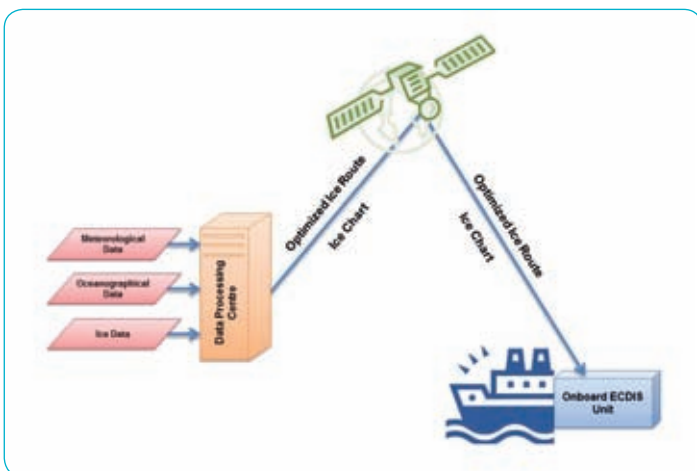


Fig. 1: Sketch of IRO-2 Ice Routing Service



Fig. 3: EM-31 mounted at R/V Lance bow

1) Hamburgische Schiffbau-Versuchsanstalt GmbH, 2) University of Hamburg, 3) OASyS GmbH, 4) Alfred-Wegener-Institute, 5) Bundesamt für Seeschifffahrt und Hydrographie

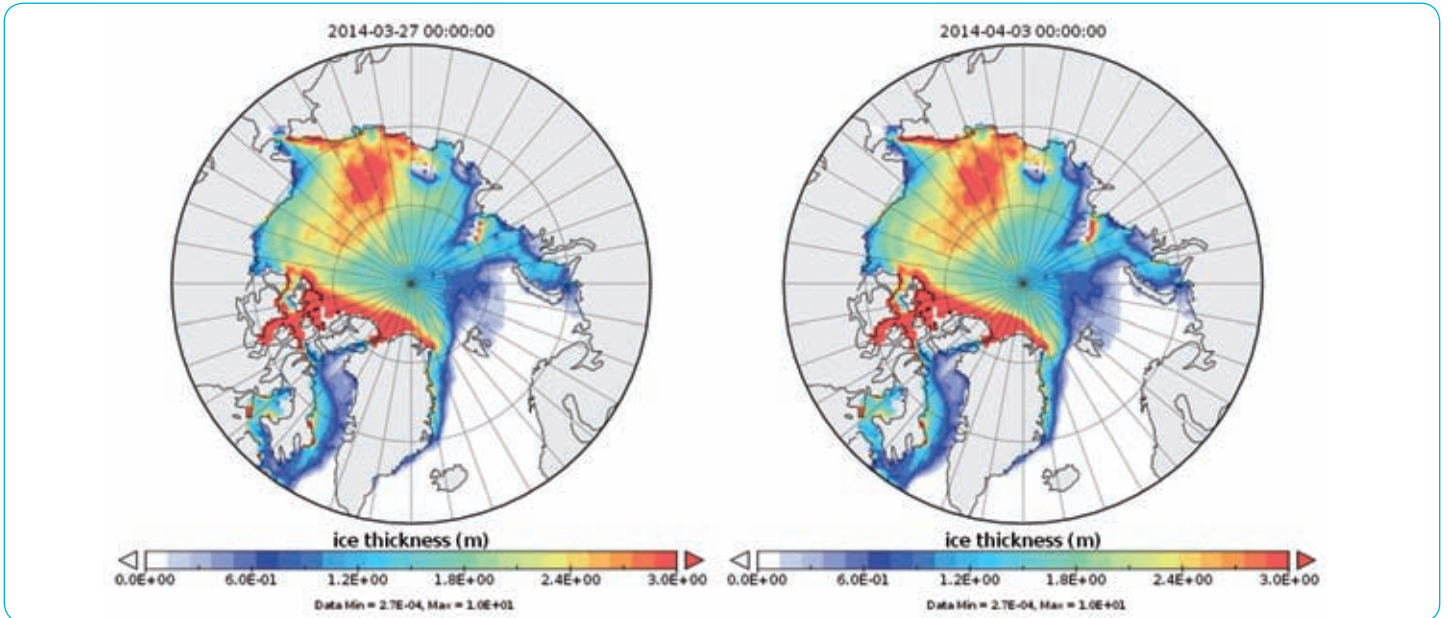


Fig. 4: The optimized initial ice thickness (m) on 2014-03-27 and the 7 day forecast on 2014-04-03

while AWI used an airplane to determine ice thickness information on a larger scale for comparison purpose with ESA satellite information(SMOS).

During the full scale trial the land crew in Hamburg, Bremen and Rostock worked on the predictions which were compiled on a ftp-server of the BSH in Rostock. This server was used as communication link onshore. Data sharing between R/V Lance and shore base, BSH, was performed using Iridium Satellite Link.

The first part of the routing optimization was an arctic-wide sea ice-ocean model delivering lateral and initial conditions for the regional coupled atmosphere-sea ice-ocean model HAMMER of the University of Hamburg. By means of a variational data assimilation system (ICEDAS) sea ice and ocean remotely sensed observations (ice concentrations, ice- and snow thicknesses and sea surface temperature) are combined with model data

through the minimization of a cost function (also called misfit function). Thereby ICEDAS is forced by atmospheric analyses and forecasts of the European Center of Medium-Range weather Forecast (ECMWF). Fig. 4 shows the initial ice thickness on 27th March 2014 (left) and the 7 day forecast (right). Sea ice and ocean observations from March 20th to 26th are assimilated.

The next element in the IRO-2 process chain is the worldwide unique sea ice forecast software HAMMER of the University of Hamburg. Hammer is a coupled atmosphere-sea ice-ocean-model using beside data from ICEDAS and ECMWF as boundary also remote sensing products like SMOS and AMSR2 as initial conditions. Fig. 5 presents a 84 hours sea ice thickness forecast together with the actual vessel track from March 20th 00:00 to 24:00.

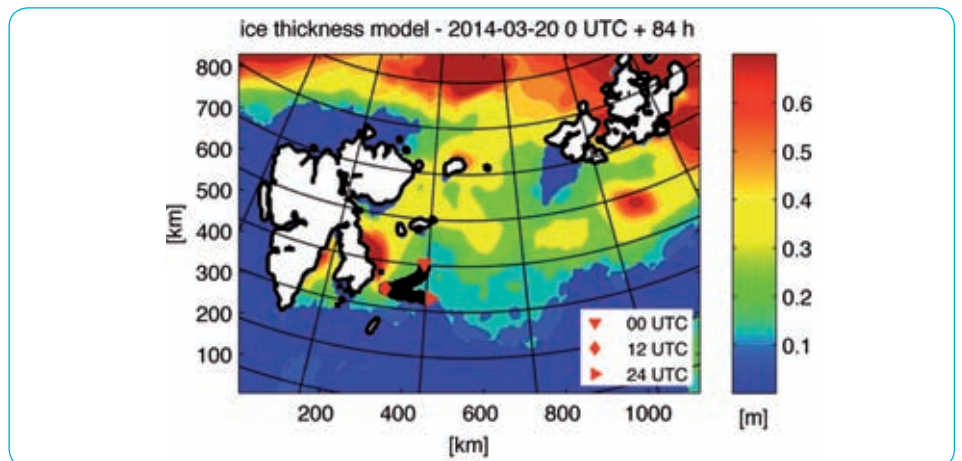


Fig. 5: Ship positions and results from an 84 hour sea ice thickness forecast

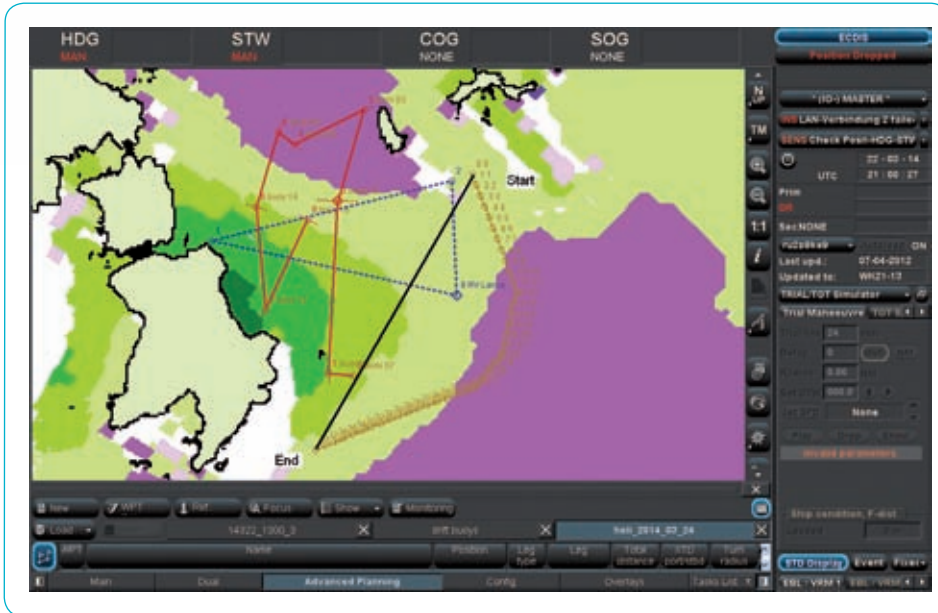


Fig. 6: Screenshot of ECDIS System on board R/V Lance showing ice thickness chart (background colors), optimized route (brown), helicopter track (blue) and drift buoy track (red)

At the end of the process chain the HSVA routing software ICEROUTE calculates time optimized routing alternatives while the BSH translates the ice forecast data into an ECDIS compatible format. This data are transmitted from the BSH shore base to the R/V Lance via the Iridium satellite link and present in overlay technique on an ECDIS system. The same link was used to send routing prediction request from Lance to shore. Fig. 6 shows an ECDIS System screen shot.

As the main goal of the trial was the validation of the system performance the real time ice thickness measurements using the EM31 mounted at the bow of Lance was of particular importance. Already during the trial preliminary analysis and assessment could be done. As presented in Fig. 7 there was a good agreement between the ice thickness forecast of the Hammer model and the real time EM31 ice thickness measurements. Differences may have two reasons:

- ➔ due to the brief analysis only a time averaging was applied to the raw EM data while it is necessary to take also area variations into account
- ➔ this revision of the HAMMER forecast model only reports convergence and divergence but is not able to forecast first year pressure ridge keel depth and frequency.

Sometimes the Lance crew requested also some challenging way points in order to navigate into hard ice conditions. Figure 5 shows such route, which led the ship towards difficult conditions ramming a first year ice ridge at noon time. As it was too hard for Lance to break this ridge the passage was continued after course change. The sea ice thickness time history presented in Fig. 8 and determined by the EM-31 contactless ice thickness sensor mounted at the bow of the Lance shows very clearly the presence of the pressure at noon time.

A good example for a successful routing optimization is presented as a screen shot from the ECDIS system in Figure 9. The background color illustrates different ice thicknesses, yellow represents thick, magenta medium and blue thin ice.

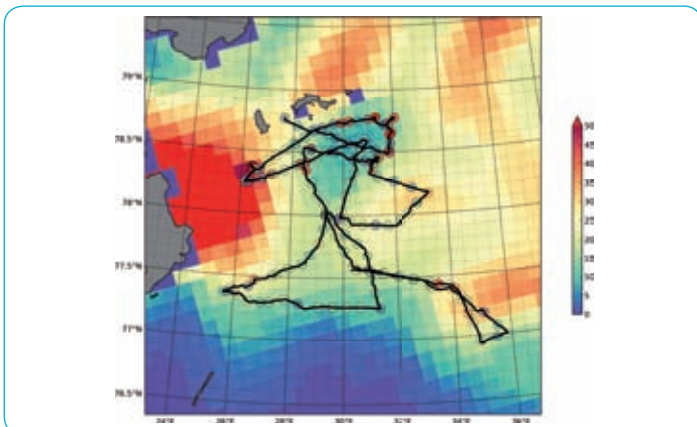


Fig. 7: Comparison of ice thickness forecast by HAMMER model and actual measurement by ship EM-31

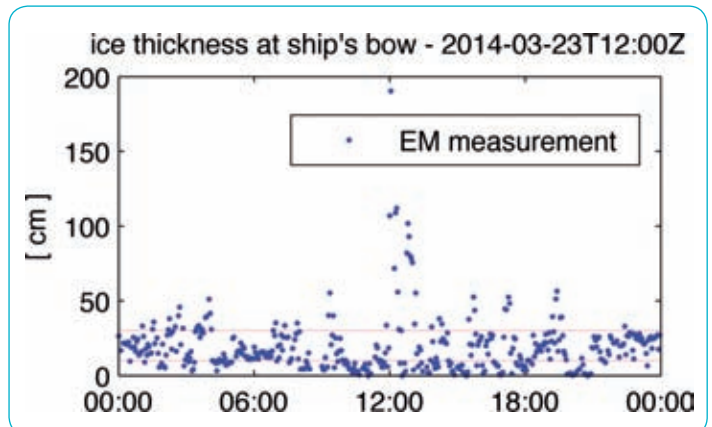


Fig. 8: Time series of sea ice thickness measured along the ship track shown in Figure 5. At noon the ship changed the course after meeting an ice ridge

R/V Lance was on standby at the location marked “Departure” and was expected to navigate to the point marked “Destination”. The route calculated by the ICEROUTE system is shown as the brown line. Following the predicted course Lance arrived at its destination at the forecasted time. In order to prove and assess the ICEROUTE System Lance tried to return from “Destination” to “Departure” using shortest distance between the both locations and passing the thick ice, blue line. At waypoint 3 R/V Lance got stuck but was able to continue the voyage after changing the course. This sample shows exemplary the effectivity of the ICEROUTE System.

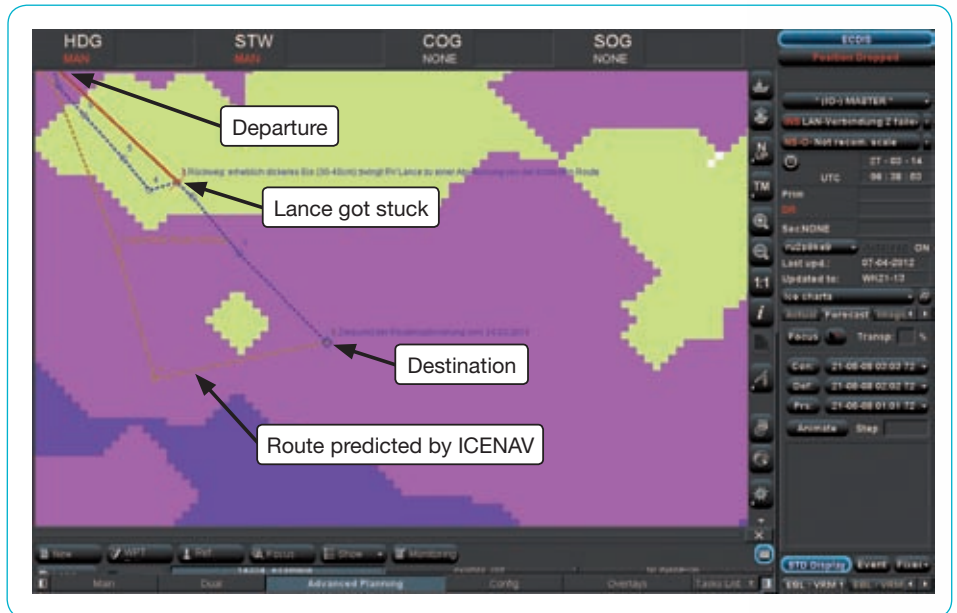


Fig. 9: Screenshot of the shortest and an optimized route by ICENAV System

Viscous Flow Supported Skeg Optimisation for an Articulated Tug-Barge Unit

by John Richards & Peter Horn

On behalf of Moran Towing Corporation of New Canaan CT, USA, an investigation of the skeg arrangement for an articulated tug-barge unit was performed. The barge aftbody is fitted with two skegs, each of which houses a ballast pump, box coolers and sea chests. The initial skeg arrangement and structural design were provided by Guarino & Cox LLC.

The purpose of the study was to optimise the alignment and/or the shape of the skegs in order to minimise their hydrodynamic resistance. Viscous flow CFD calculations

were employed as a design analysis tool. No model tests were planned.

The calculations were carried out for a speed of 11.0 knots for one loading condition of the tug (design draught) and two loading conditions of the barge (ballast and full load). All calculations were performed with the tug and the barge connected in a fixed condition. The tug was at even keel and the barge was set to a condition with a realistic stern trim based on the operation profile of the vessel.

Due to budget and time constraints, the calculations were performed with free

surface but without taking dynamic trim and sinkage into account. This approach was considered to be fully adequate for determining the effect of the skegs on the vessel's resistance.

The procedure to be followed for the optimisation was agreed upon between HSVA and Moran Towing before commencing work. In a first step the tug-barge unit was investigated without skegs (Figs. 1 and 2). The figures show the bottom of the barge in way of the skegs viewed looking ahead from the starboard side. In order to better visualise the flow in the notch the tug has been made translucent.

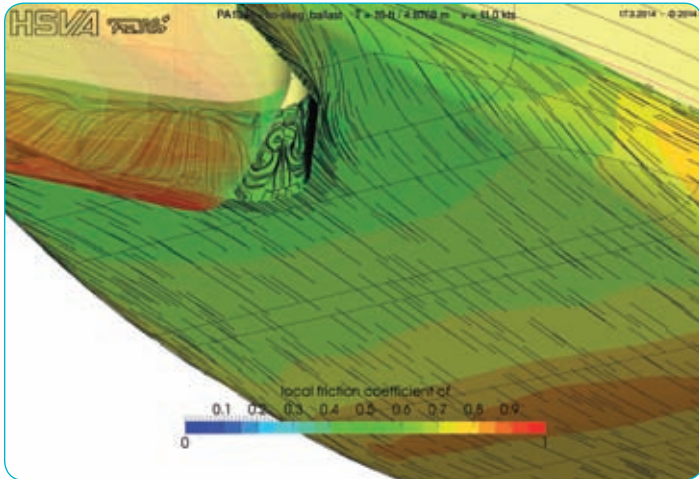


Fig. 1: Ballast loading condition – without skegs

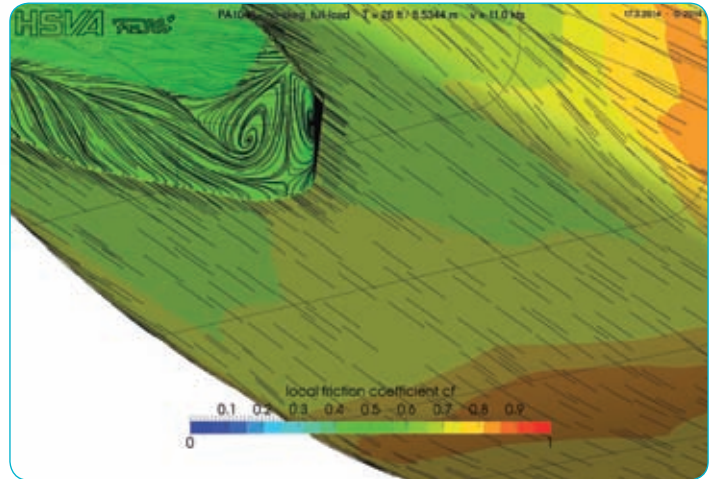


Fig. 2: Full load condition – without skegs

The results of these calculations gave insight into the general flow over the tug-barge unit in way of the barge aftbody but without any disturbances to the flow caused by the skegs.

The second step was to do the calculations for the tug-barge unit with the initial skegs fitted (Fig. 3). In a final step an alternative skag geometry as proposed by HSVA was investigated (Fig. 4). When designing this alternative skag certain constraints on the position of the skegs and also on the

interior arrangement of the pump and box coolers had to be met.

The calculation results showed that at full load draught the trailing end of the skag should be turned slightly inboard to be exactly in line with the local flow. However, there is an opposite trend visible at ballast draught. This is caused by the displacement of the flow in an outboard direction upstream of the tug. Based on these results it was decided to retain the original skag alignment and only to modify the shape.

The calculations also produced quantitative results for all conditions investigated, and the concluding finding was that the overall resistance of the tug-barge unit can be reduced by about 2% at both draughts by implementing the proposed skag modification.

This study shows that performance improvement can be achieved by paying attention to details which at the outset may not appear to be so significant.

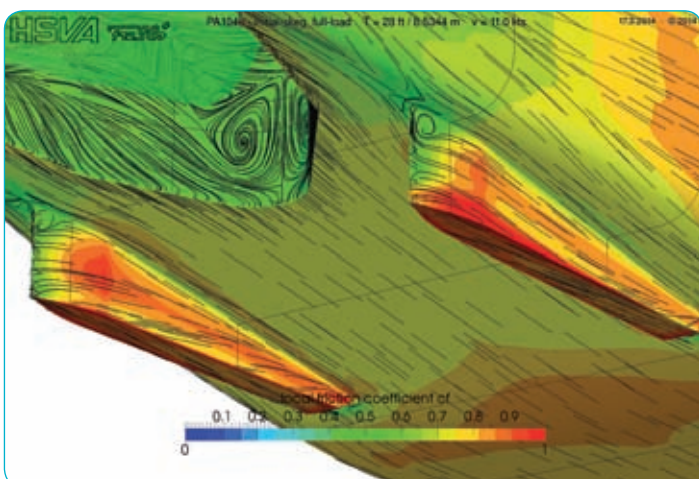


Fig. 3: Full load condition – with initial skag geometry

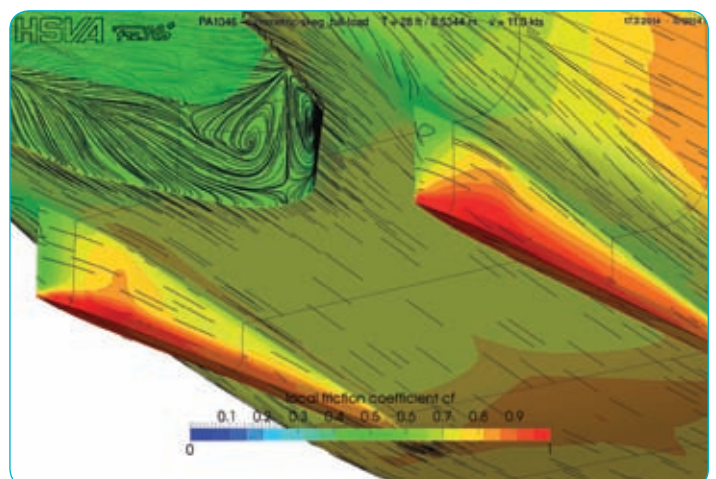


Fig. 4: Full load condition – with modified skag geometry

Towards Ships with Low Wave Drag

✍ by Lars-Uve Schrader

Naval architects have been dreaming of designing waveless ships for more than one century. Striving for this ideal constitutes an optimization problem: “Find a hull form with minimum wave creation.” To pursue this optimization task, HSVA recently joined forces with three partners from industry and academia within the research project **No-Welle*** (Fig. 1).

No-Welle sets out to minimize the wave resistance of ships by modern shape optimization techniques. In the language of optimization, wave drag represents the objective while the hull shape constitutes the control of the optimization problem. Objective and control are linked via the shape sensitivity, a measure for the effectiveness of the control with regard to the objective. Consider the following optimization task for illustrative purposes: “Find a bulbous-bow shape minimizing the hull resistance.” The shape sensitivity (Fig. 2) indicates the local deformations of the bulbous bow that will lead to reduced resistance of the ship.

There are different ways of computing shape sensitivities on ship hulls. In the research project **FORM-PRO** (2009-2012), HSVA and their partners pursued the very promising path of adjoint shape optimization [1]. To this end, the in-house RANSE solver **FreSCo+** was augmented by its adjoint counterpart **adFreSCo+** [2]. In the adjoint framework, the shape sensitivity with respect to a certain objective is efficiently computed by a sequence of direct and adjoint flow simulations. The strength of this approach lies in the independence of the computational effort from the number of hull design variables: Every single node of the hull surface mesh can be allowed as a control parameter without compromising the computational

efficiency. In **FORM-PRO**, the **(ad)FreSCo+** package was embedded in an iterative process chain, in which the hull deformations were executed within the CAD design environment **FRIENDSHIP-Framework** (Fig. 3). This toolbox was successfully used for the design of an asymmetric stern of a bulker, resulting in largely improved propulsive efficiency [3].

For the purpose of **No-Welle**, the design chain will be enhanced by a free-surface treatment in order to incorporate wave effects into the hull shape optimization. To this end, **adFreSCo+** will be complemented with an adjoint VOF equation (cf. Fig. 3) for the tracking of the adjoint wave field around the ship. Clearly, this step is mandatory for the example of bulbous-bow optimization mentioned above. In **No-Welle**, HSVA will use the enhanced adjoint method for shape optimization of the wave-making and wave-reducing parts of ship hulls such as bulbous bows, fore and aft shoulders and trim wedges.

***No-Welle** is funded by the Federal Ministry for Economic Affairs and Energy of Germany (BMWi).



Fig. 1: The **No-Welle** research consortium consists of Voith Turbo Schneider Propulsion GmbH, Hamburg University of Technology (TUHH), FRIENDSHIP SYSTEMS GmbH and HSVA (coordination).

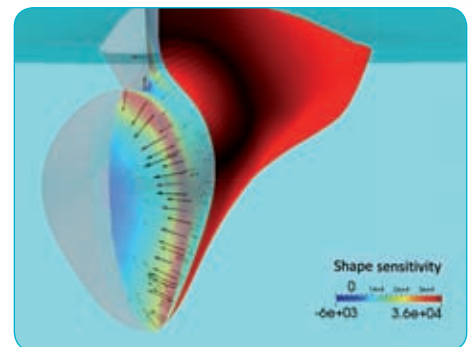


Fig. 2: Shape sensitivity with respect to the hull resistance on the bulbous bow of a PANMAX container vessel. The arrows indicate the deformations of the bulb that will lead to reduced resistance. In this example, the free surface is included in a static manner as a boundary of the CFD domain only. In **No-Welle**, the free-surface computation will be dynamically linked to the adjoint shape optimization methodology.

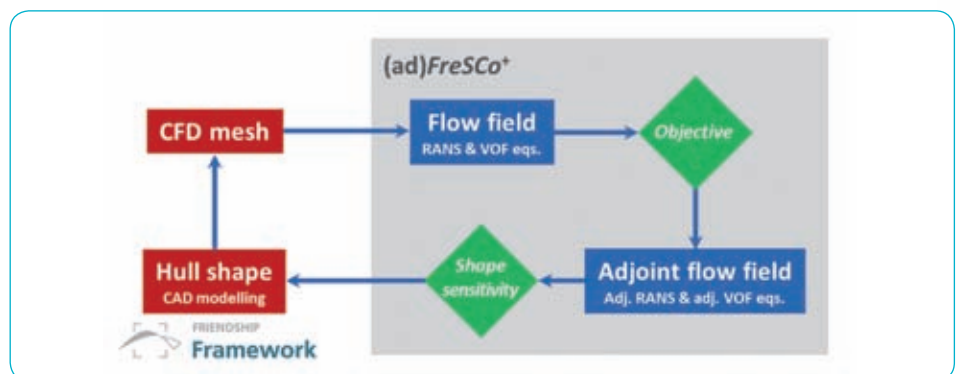


Fig. 3: Iterative process chain for CAD-based adjoint shape optimization. In **No-Welle**, direct and adjoint free-surface computations will be incorporated into the optimization loop.

[1] Brenner, M., Harries, S., Wunderlich, S., Kröger, J., Stück, A., Rung, T., Gatchell, S., Schrader, L.-U., Marzi, J. 2012 FORM-PRO – Hydrodynamische Optimierung von Schiffen mit aktiver Propulsion. Report Series Projektträger Jülich „Statustagung Schifffahrt und Meerestechnik“ 2012, 65-83 (in German).
 [2] Stück, A. 2012 Adjoint Navier-Stokes Methods for Hydrodynamic Shape Optimisation. Technical Report Series “Schiffbau“ 661, Hamburg University of Technology (TUHH).
 [3] Marzi, J., Gatchell, S. 2013 Form-Pro to Revive the Asymmetric Single-Screw Ship. HSVA Newswave 2013/1, 12-13.

Measurements of Wave Added Resistance in Oblique Seas

by Petri Valanto

Towing Arrangement

In the framework of the research project PerSee (Performance in Seaway) the HSVA has carried out a large number of measurements on wave added resistance in regular waves in seven wave directions between 180° and 0° of ship heading. In the tests it was necessary to use a new towing arrangement, which allows the ship model as free motions in oblique seas as possible, but makes it simultaneously possible to measure the towing resistance.

The ship model is towed with a vertical towing pole located in the middle of the ship.

A vertical guiding pole at the bow controls the ship model direction. For accurate measurement of the towing force and the side force, each pole is connected to the model with a purpose-built articulated force balance.

The ship motion components roll, pitch, and heave are completely free. The surge, sway, and yaw – components are restrained with suitably soft springs allowing the cyclic motions of the model in seaway, but keeping it softly on its course and position.

For accurate measurement of wave added resistance the ship must be able to execute roll motions freely in all wave directions. For this it is important to have the roll

axis of the ship model in the correct height above the baseline, also when the ship model is connected to the towing system. This is realized with the two articulated force balances.

The towing arrangement in Figure 1 allows to carry out measurements on the resistance of ship hulls with different bow forms, as in Figure 2, also in oblique seas, thus giving impulses to ship hull design and optimisation. Second, it allows to study the efficiency of the propulsion in seaways of all wave directions. We are convinced that the new towing arrangement will help in designing ship hulls for optimum performance in seaway and in choosing the best propulsion point for a chosen ship design.

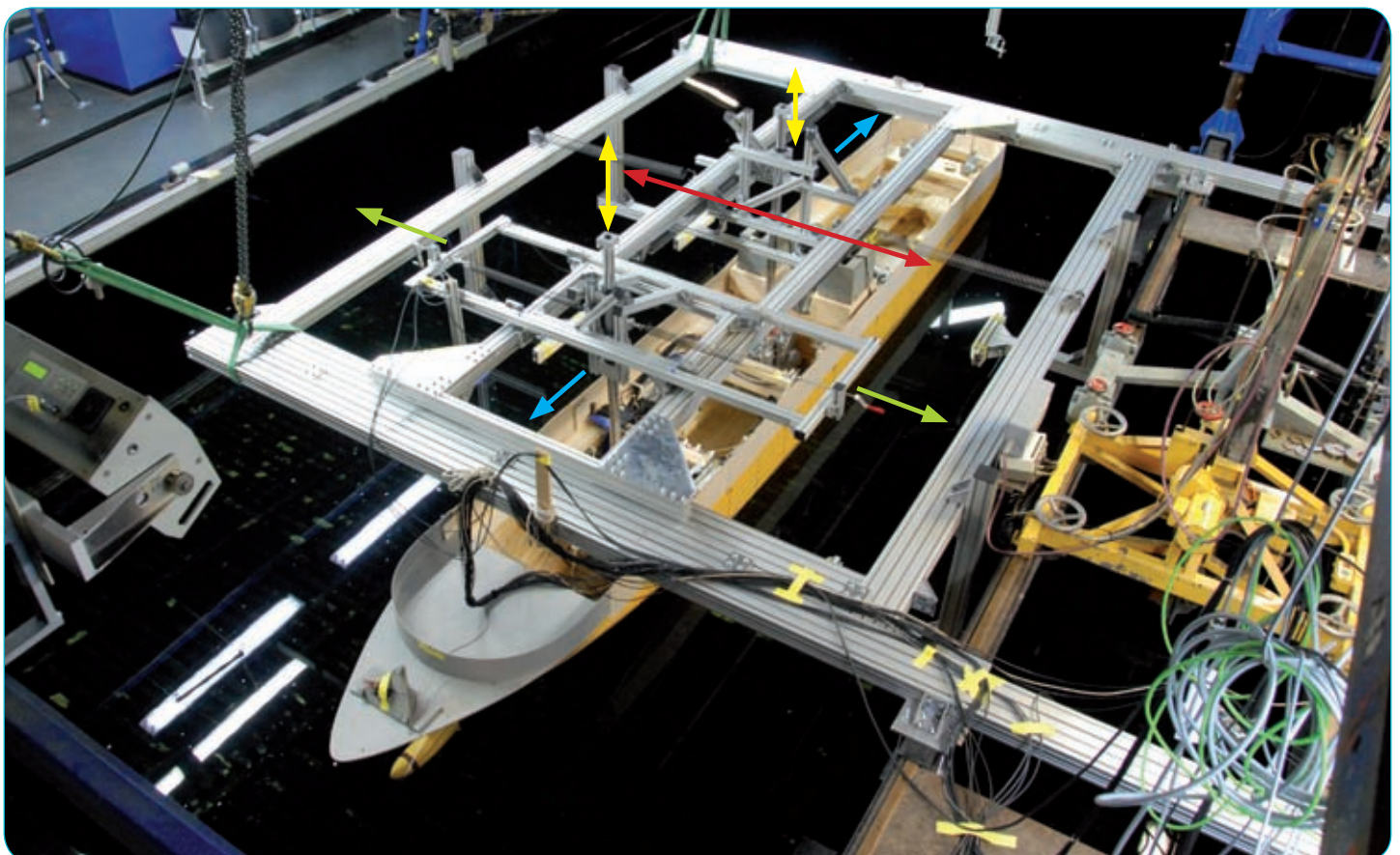


Fig. 1: Trial version of the new towing arrangement for oblique seas in the HSVA large towing tank. The arrows show the direction of the movement of the different components of the system.

Test Program

The towing tests in regular waves were carried out with the model of a 221 m long cruise ship design by Meyer Werft. The model was equipped with rudders, propeller shafts, shaft brackets, and bilge keels, but with no bow thruster openings.

The main goal of the tests was to measure the RAO's of the wave added resistance on the whole wave length range in seven wave directions between head and following seas. For each wave direction 11 – 15 resistance points were measured to get complete RAO-curves. Most of the tests were carried out with the full scale speed of 21 kn, a small number with a slower speed of 15 kn for purposes of comparison.

The two wave makers in the HSVA towing tank, (1) The K&R wave maker at the end of the towing tank and (2) The Side Wave Generator in the middle of the long side of the tank were used to cover all required wave directions. The tests were carried in regular waves having wave length to ship length (λ/L) –ratios between 0.18 and 2.5. The corresponding wave periods varied between 4.81 s and 18.99 s in full scale.

Test Results

The wave added resistance R_{AW} is obtained as the difference between the total resistance measured in waves R_{TMW} and the total resistance measured in calm water R_{TMC}

$$R_{AW} = R_{TMW} - R_{TMC}$$

The dimensionless added resistance coefficient C_{AW} becomes

$$C_{AW} = \frac{R_{AW}}{\rho g \zeta_A^2 B^2 / L_{PP}}$$



Fig. 2: Two different bow forms of the hull were tested and compared.

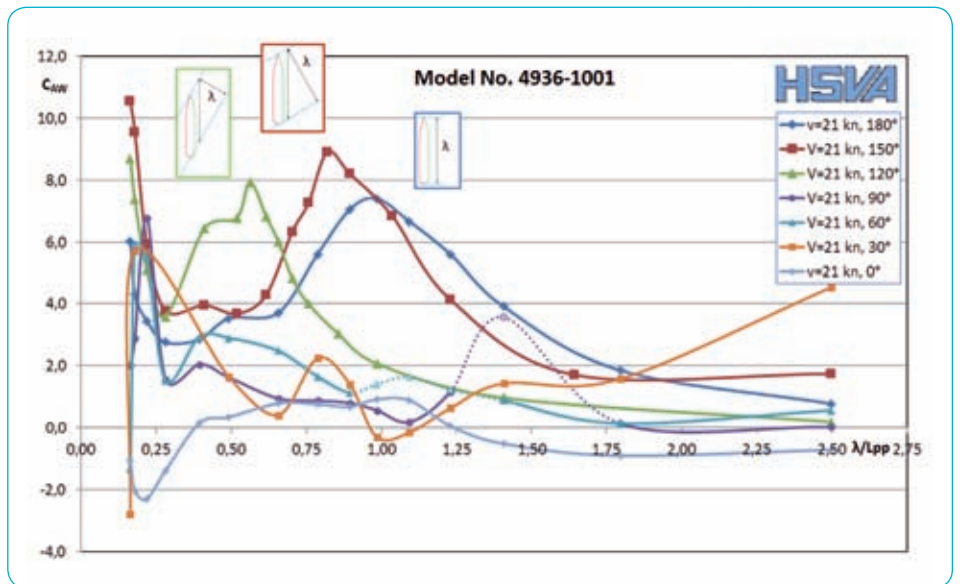


Fig. 3: Measured C_{AW} -curves for the wave added resistance as a function of the λ/L_{PP} -ratio

where R_{AW} is the wave added resistance, ρ the density of the tank water, g the acceleration of gravity, ζ_A the measured wave amplitude, B the breadth of the ship model at the design waterline, and L_{PP} the length between

perpendiculars. Figure 3 shows RAO-curves of the coefficient C_{AW} as a function of the λ/L_{PP} -ratio, where λ is the wave length. The measured points are directly connected with splines without any smoothing of the

curves, which would reduce deviations due to potential scatter in the raw experimental data. The small sketches above the curves are color coordinated and they show how the ship lies in the waves having different encounter angles with the ship. With the increase of the relative angle between the direction of the wave propagation and ship direction the peak of the RAO moves toward shorter and more frequent waves in the oceans. Not only are the peak values of the C_{AW} in bow quartering seas higher than in head seas, but these peaks are also reached in shorter and more common waves than the peak values of the RAO for C_{AW} in head seas. All this emphasizes the relative importance of the wave added resistance encountered in bow quartering seas.

At very short wave lengths the C_{AW} values increase steeply, which is quite common. However, at the area of very short waves the accuracy of the measurements is at the lowest, which should be kept in mind. In beam (90°) and stern quartering ($60^\circ, 30^\circ$) seas the C_{AW} values are in general lower than in bow quartering seas, but by no means negligible. The curves contain some humps or elevations, which at the first look appear as if caused by some scattered, measured data points. In stern quartering seas these local peaks are found in same wave lengths as the peaks in bow quartering seas.

Also the RAO's of the ship model motions were measured in the tests. A careful study of these curves shows that many of the humps and hollows of the non-dimensional wave added resistance C_{AW} -curves coincide with the high and low values of the RAO-curves of the ship motions. Thus what at first look may have looked as data points scattered off the correct path of the C_{AW} -curve, are in fact properly measured data points simply reflecting high or low values of the C_{AW} due to certain ship rigid body

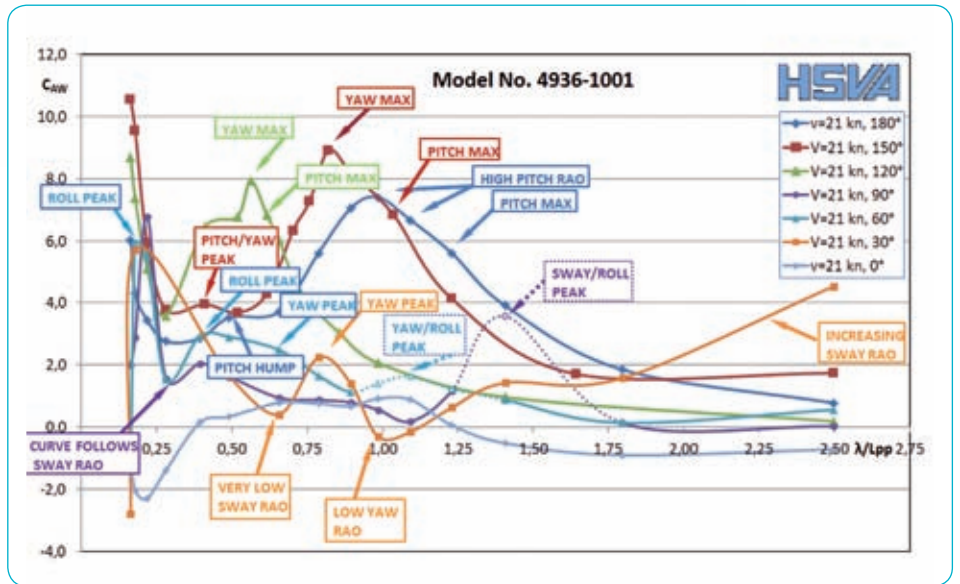


Fig. 4: Measured C_{AW} -curves for the wave added resistance. The positions of the peaks or low values of the ship motion RAO's are indicated in the figure with color coordinated arrows and labels. The dotted parts of the curves may be influenced by the towing frame.

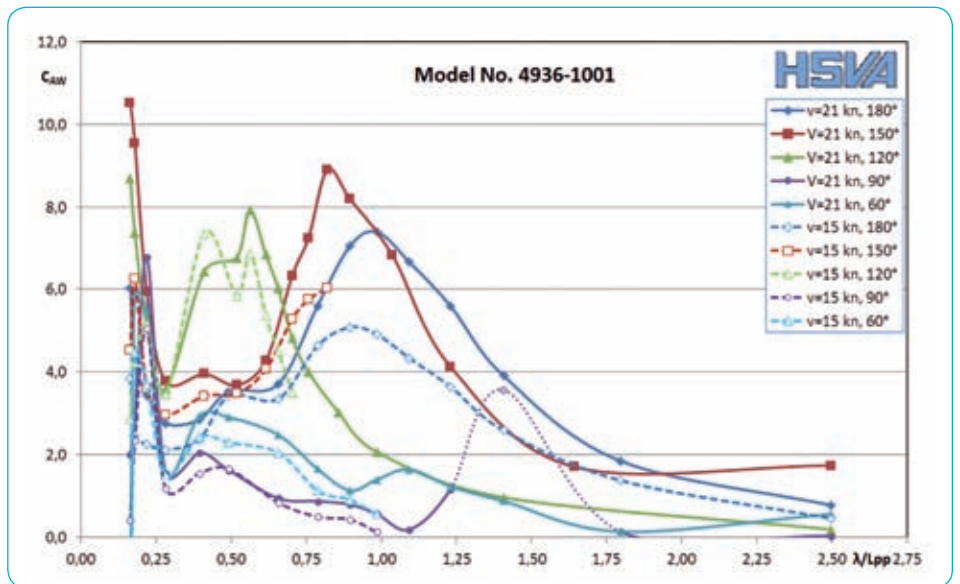


Fig. 5: Measured C_{AW} -curves for the wave added resistance at different speeds

motion components. The measured C_{AW} -curves are shown once again in Figure 4, with labels indicating the lows and highs of the ship motion RAO's. It should be obvious that increased ship motions lead also to

elevated values of wave added resistance. The comparison between the measured wave added resistance and the ship motion components helps also to identify the possible influence of the towing frame

on the measured resistance values, if any, which further improves the reliability of the measured data.

Also the effect of ship speed on the wave added resistance was studied. Beside for the ship speed 21 kn, the C_{AW} -values were also measured at the speed 15 kn, for the λ/L_{PP} -range 0.16-1.0 and the wave directions 180°, 150°, 120°, 90°, and 60°, as shown in Figure 5. Following observations can be done:

As expected the C_{AW} -values increase with speed. Particularly clear is this increase at the λ/L_{PP} -range around one, where several curves reach their maxima. Interesting is also the area of shorter, more common waves, where for many wave directions the C_{AW} -values increase only relatively little with speed. As the ship speed in calm water is reduced from 21 kn to 15 kn, the ship resistance drops coarsely to a half, whereas the wave added resistance appears to drop usually much less than 20 percent. The consequence of this is that the relative part of wave added resistance of the total resistance in shorter waves at speed 15 kn is much higher than at speed 21 kn. If we consider sea margin, which must also cover the wave added resistance, it is clear that it should not be taken as directly proportional to propulsion power or ship speed, but has a more constant character.

Comparison of two Bow Forms

Figure 6 shows the measured C_{AW} -values for the two bow forms. In very short waves, at the λ/L_{PP} -ratio of 0.16 – 0.28, the vertical bow form (-2101) without bulb yields lower resistance values than the original cruise ship bow (-1001) in wave headings 180° and 150°. When the waves become longer, this difference becomes less clear, eventually the tendency can reverse.

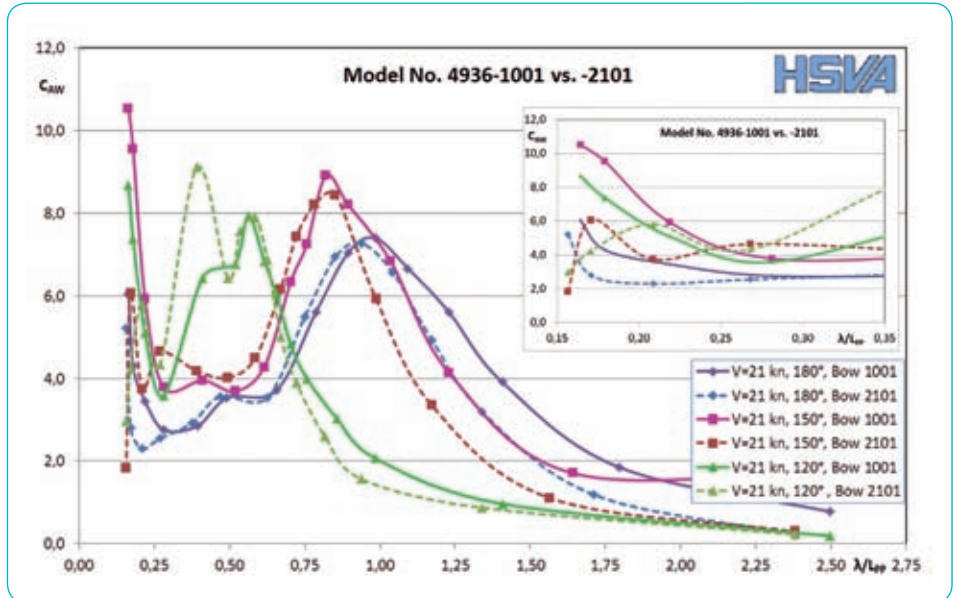


Fig. 6: Measured C_{AW} -curves for the wave added resistance for two bow forms. The plot on the right shows the curves at very short wavelengths.

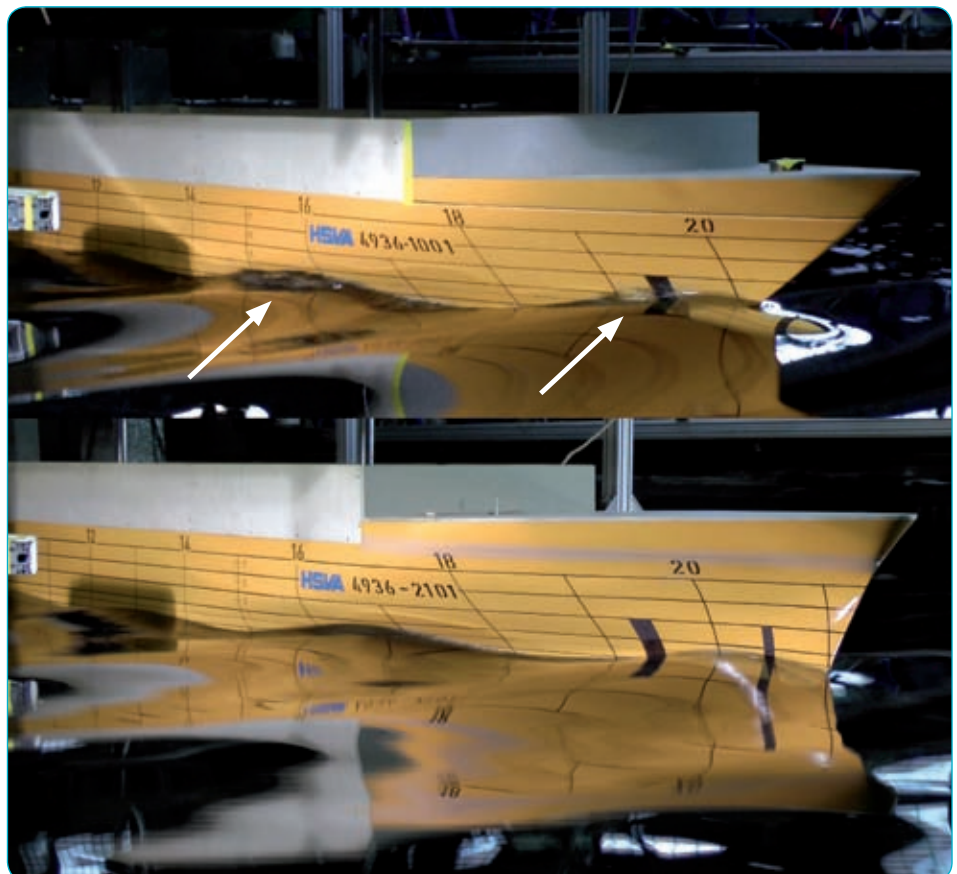


Fig. 7: Breaking (arrows) and non-breaking waves at the bow of the model No. 4936-1001 (up) and No. 4936-2101 (down), respectively, in head seas. The speed is 21 kn and the λ/L_{PP} -ratio 0.18.

The wave pattern along the ship bow in regular short head waves is shown in Figure 7 for the two bow forms. The original cruise ship bow (-1001) on top has a bulb and more inclined frames in the bow. The vertical bow without a bulb (-2101) has more vertical frames in the bow. Notice the difference in the wave pattern between these two bow forms. The wave system with the vertical bow (lower figure) shows a very smooth behavior, whereas the waves along the original bow (upper figure) all break as a result of the wave elevation. It can be assumed that this is an important mechanism causing higher wave added resistance in short waves with bow forms having inclined frames, in comparison to bow forms with more vertical frames.

Conclusions

The highest wave added resistance values were not measured in head seas, but in bow quartering seas.

Practically all ship motion components in a large range of wave lengths have a clear effect also on the wave added resistance.

The accurate determination of the propulsion point of a ship design in real seaway conditions should benefit from the resistance measurements in a wide range of wave directions and wave lengths.

The comparison between the two bow forms -1001 and -2101 shows that it is possible to design an alternative, vertical bow without a bulb having equal calm water resistance, a

slightly lower resistance in short waves, and about equal resistance in waves about the ship length. Thus for a cruise ship sailing much in shorter waves the vertical bow with steep frames is a very interesting design alternative.

For a cargo ship such a vertical bow would have the additional advantage that the bow without a bulb would be less draught dependent than the classical bulbous bow form.

Based on this study the highest resistance in seaway is experienced in bow quartering, in more frequent seas states than those leading to maximum resistance in head seas. From the point of view of the actual energy efficiency and savings in the fuel consumption of the ship, it is not enough to study only the head sea condition.

Reliable Prediction of Ship Motions in Seaways for Complex Hullforms

 by Jan Peter Voß

A reliable prediction of ship motions in seaways is a topic of high interest in the ship-design process. Heavy ship motions and induced forces in seaways can lead to damage or loss of cargo, physical injuries of crew-members or extensive damages to the hull structure up to the final loss of the ship. Related to these consequences the highest threat results from high roll motions. The feasibility of occurrence of high roll motions depends on shipping route and the encountering seaway, loading conditions and hullform.

The prediction of ship motions in seaways is nowadays typically based on model tests. For the cases for which no model tests are conducted, the roll damping coefficients for single-hull ships can be estimated according to the work of BLUME [1] or IKEDA [2], which is based on a wide range of model tests performed in the 1970s. However, for modern hullforms (especially multi-hull ships or ships with flat transom) these roll damping coefficients are more a rough guess.

Numerical methods can be used to generate results with good accuracy. At HSVA, both non-viscous and viscous flow computations can be performed to predict the seakeeping

behaviour of ships. With respect to computational effort, non-viscous, potential theory based strip-methods are preferred over viscous RANS-codes. However, for the calculation of roll motions with potential flow (this holds for other potential methods as well)-methods the roll damping of the hullform must be known. The roll damping is not only affected by the shape of the bare hull but also by appendages, such as bilge keels or fins.

With the in-house strip-method STRIP, as a part of the Uthlande framework, ship motions can be determined for a given seaway spectrum with low computational

costs, but is very sensitive to the correct choice of roll damping coefficients. The in-house RANS-Code **FreSCo+** needs higher computational effort, but it gives a satisfying accuracy for complex hullforms. The roll damping coefficients need not be specified, because the ship motions are directly deduced from the viscous flow field.

A “combined-method” includes a numerical roll decay test with the viscous flow solver **FreSCo+** and the simulation of ship motions using the strip method. First, **FreSCo+** performs the roll decay test for zero speed on a ship geometry with all appendages. The theoretical roll damping curves from [1] and [2] are adjusted, and applied in STRIP for the calculation of ship motions in seaways.

The combined-method was tested for a tug vessel in the context of the BMWi funded project TUG-Design. The aim of TUG-Design is the development of a seakeeping prediction tool for ships with small, full hull forms. Project partners of HSVA are the Technische-Universität Hamburg-Harburg and Voith Turbo Schneider Propulsion GmbH.

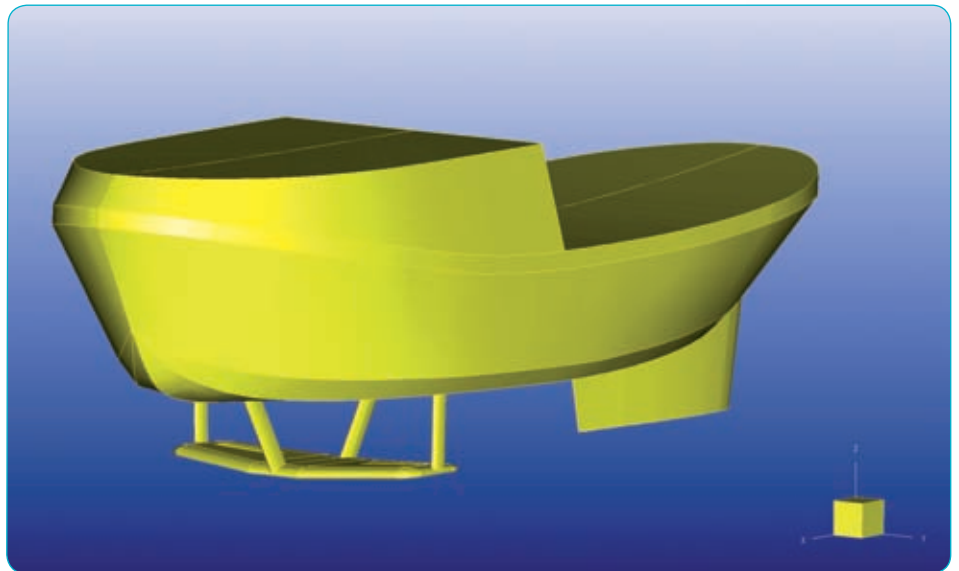


Fig. 1: Tug geometry with appendages

The hullform of the tug vessel is shown in figure 1. The hullform is characterized by a full shape, a large fin to ensure roll stability and a horizontal, profiled plate with struts to cover the Voith-Schneider Propellers. On closer inspection of the ship geometry it's assumable that the roll damping is highly affected by flow separation at struts and fin.

In the numerical roll decay test an initial roll angle of 20 degrees was applied and twelve roll periods were simulated. The history of the roll motion is plotted in figure 2 and the logarithmic decrements are plotted over the mean roll amplitude in figure 3. These show that the roll damping is highly uniform for a wide range of roll angles, with less scatter than in model tests.

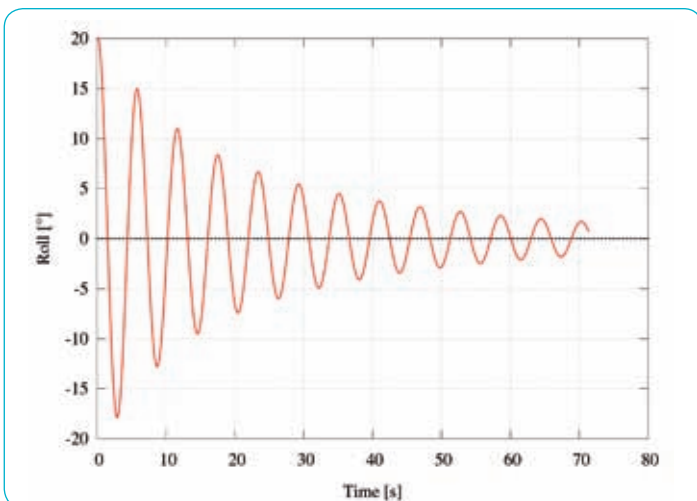


Fig. 2: Time history of roll motion in the numerical roll decay test

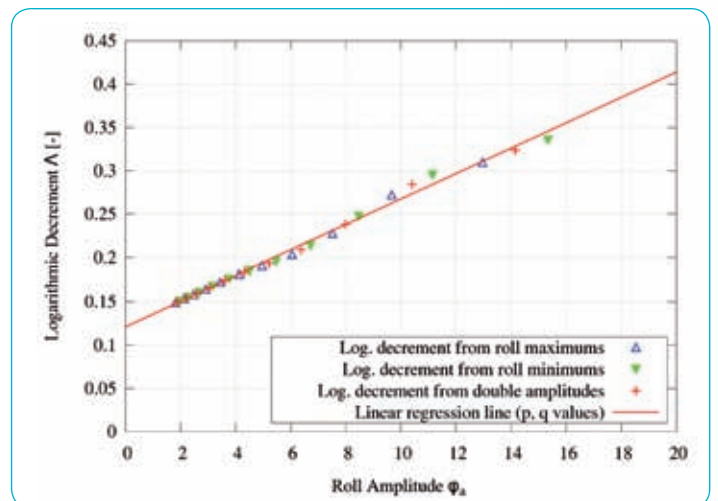


Fig. 3: Logarithmic decrement derived from roll amplitudes

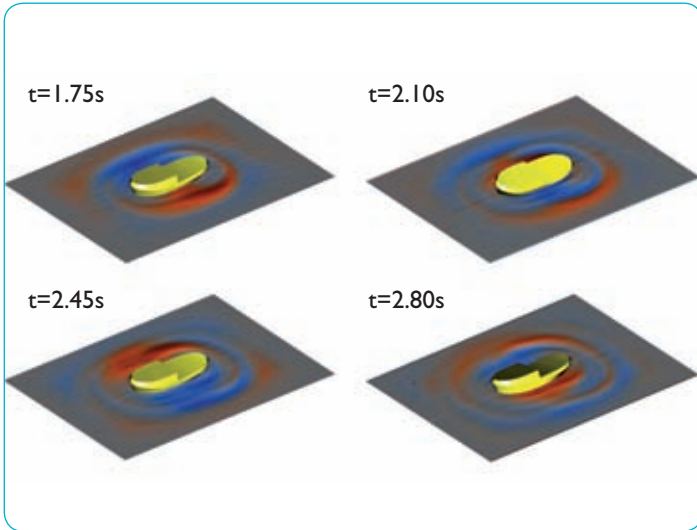


Fig. 4: Snapshots from numerical roll decay test

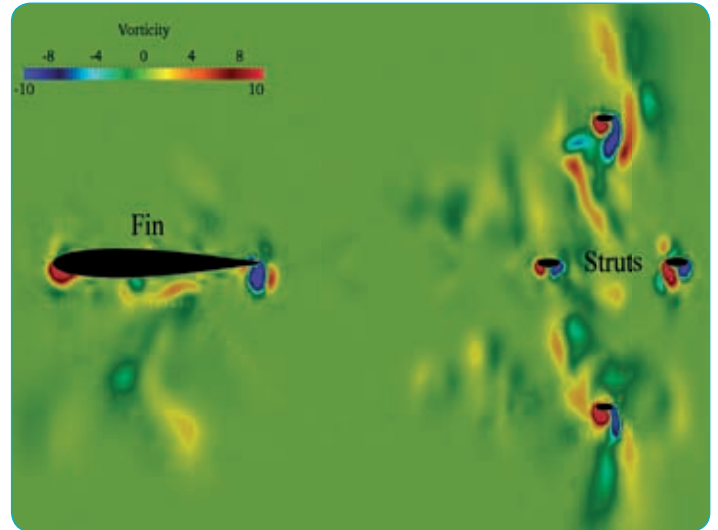


Fig. 5: Vorticity in a horizontal plane, intersecting fin and struts during roll motion

Figure 5 shows the flow-field of the roll decay test in a horizontal plane, intersecting struts and fin, during the second roll period. At the edges of struts and fin, flow separations with high vorticity can be observed.

Figures 6 and 7 show the Response Amplitude Operators (RAO) for encounter angles of 90 and 135 degrees, respectively.

Close to the resonance frequency, ω_R , the computation with roll damping according to BLUME overestimated roll motions, whereas the IKEDA model underestimated roll motions, while for low and high wave frequencies, the results are in accordance with model tests. The newly developed combined-method using **FreSCo+** roll damping coefficients, however, shows

accurate results for the entire frequency range. Combining the advantages of both viscous and non-viscous methods, a flexible, accurate and efficient method can be obtained. From this complex case, we conclude that roll damping coefficients computed with **FreSCo+** show promise for all practical purposes.

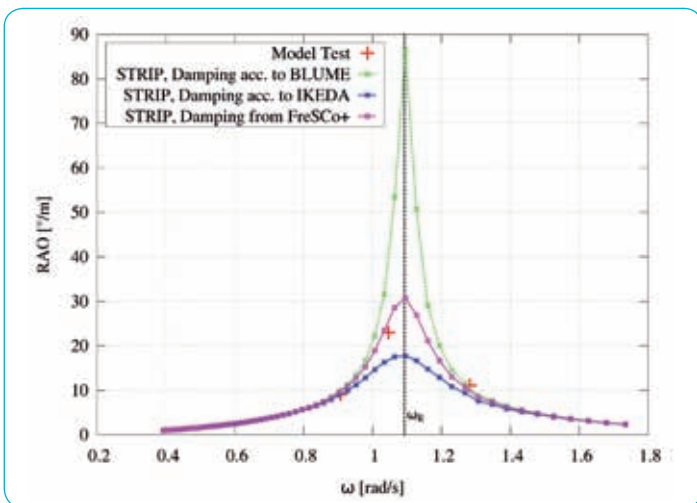


Fig. 6: RAO for roll motion in regular waves and encounter angle of 90 degrees

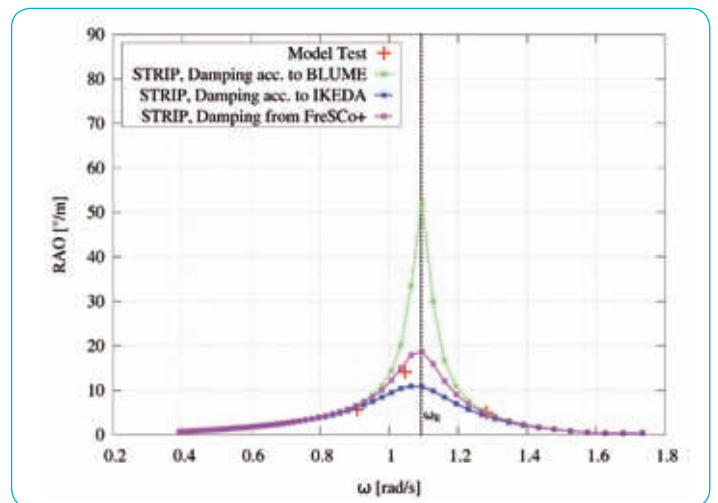


Fig. 7: RAO for roll motion in regular waves and encounter angle of 135 degrees

[1] Blume P. Experimentelle Bestimmung von Koeffizienten der wirksamen Rolldämpfung und ihre Anwendung zur Abschätzung extremer Rollwinkel; Schiffstechnik Bd. 26, 1979.
 [2] Ikeda Y., Himeno Y., Tanaka N. A Prediction Method for Ship Roll Damping; Report of Department of Naval Architecture, University of Osaka Prefecture, No. 00405, 1978.

TARGETS achieved



by Jochen Marzi

In March 2014 the EU – project TARGETS – Targeted Advanced Research for Global Efficiency of Transportation Shipping – concluded with a series of workshops held in Athens and London. Led by HSVA, project partners presented the main results achieved during the last three years to an interested audience from shipping, ship design and equipment manufacturers. For more information on the workshops see: <http://www.targets-project.eu/news.html>

Energy efficiency and environmental consideration are today's driving force for ship operators and ship builders alike. IMO's 2nd Green House Gas studies published in 2009 indicated a substantial contribution to worldwide CO₂ emissions from shipping already now and the forecast is that by 2050 between 12 to 18% of global CO₂ emissions would stem from shipping operations if there was no immediate measure. As a reaction IMO introduced a set of measures including the well-known Energy Efficiency Design Index (EEDI) in 2013 and the corresponding operational index (EEOI) as well as the SEEMP. The foundation for the development of these indices was a statistical analysis of ship operational performance, rather than a dedicated analysis of the actual energy consumption of individual ships.

To provide an alternative to these "hard coded" rules the TARGETS project, introduced in NewsWave 2011/2, developed an advanced methodology to provide substantial improvements to the overall ship energy efficiency by adopting a holistic approach towards the energy generation, transformation and storage (including unconventional sources) onboard. This resulted in a Dynamic Energy Model (DEM) for cargo vessels that integrates component-

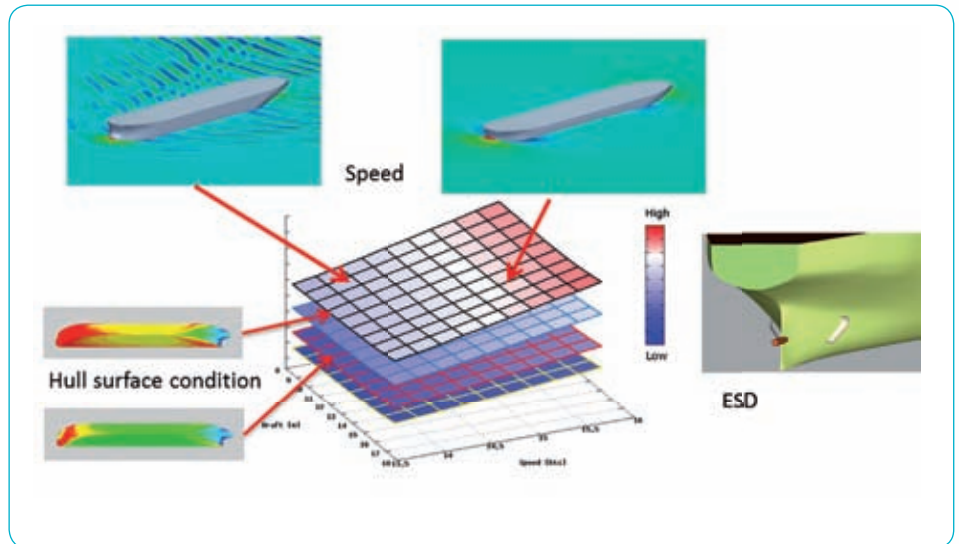


Fig. 1: TARGETS hydrodynamic model

based knowledge of ship resistance and propulsion, auxiliary energy transformation and transmission at ship-level.

As TARGETS focuses particularly on cargo vessels, hydrodynamic effects are typically the prime cause of energy consumption. In contrast to passenger ships or other complex vessels where e.g. hotel loads and consumption from other auxiliary systems can be significant, cargo vessels use up to 85% of all practically available energy for propulsion. Of course, this excludes all internal losses in a combustion engine which are not part of the present considerations. The importance of hydrodynamic effects puts resistance and propulsion analysis and optimisation at the core of energy modelling for cargo vessels and, hence, explains HSVA's avant-garde role in the project.

Starting from a comprehensive background of typical analysis tools used in ship design analysis and optimisation, the TARGETS project allowed for further improvements to the in-house RANS code **FreSCO+**,

evolving it into the main work horse for complex investigations.

Throughout the TARGETS project, HSVA performed many resistance and propulsion computations for a wide variety of ship types and operating conditions.

The computation results, in the form of response surfaces in Figure 1, serve as essential components of the DEM. A dataset starts with the performance for an initial hull form over a complete operational profile, taking the foreseen speeds, drafts and trims into account. From this, an optimisation can provide possible hull modifications at design stage using the adjoint solver included in **FreSCO+** as well as conventional methods. The computations also indicate the best performance points for an existing ship over a given route, leading to significant savings in fuel costs and CO₂ emissions.

Faithful to the overall concept of the project, energy modelling and optimisation is not limited to the design of a new vessel but shall

be applicable also to the existing fleet. The system allows for future modifications, such as retrofitting Energy Saving Devices (EDS), as well as prediction of increased resistance due to hull surface quality (i.e., fouling). A bulbous bow optimisation performed for a container ship is shown in Figure 2.

In the context of the TARGETS DEM the effect of trim and speed variation can be considered also during operation. An optimisation in form of a journey planner allows for improved performance based on a given set of parameters, e.g. environmental conditions and arrival time.

The work undertaken in TARGETS provides new technologies for optimising energy consumption of ships and a new approach

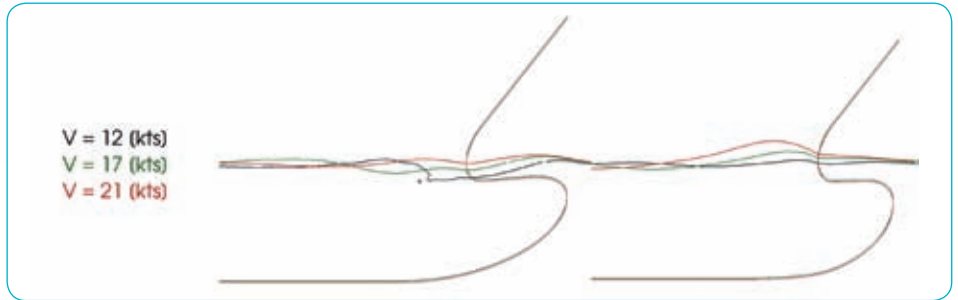


Fig. 2: Wave cuts for a bulbous bow optimisation before (left), after (right)

to assess the energy efficiency by a direct approach, using first principles tools. The approach and tools form the basis for life-cycle energy management with focus on design, operation and retrofitting. The results demonstrate considerable potential for having in place a more systematic and

scientific approach to determine the Energy Efficiency of Ships.

The research performed in the TARGETS project is partly funded by the European Commission under Grant Agreement 266008 as part of the 7th Framework Surface Transport programme

Sea Trial Procedure Updates for EEDI Verification

by Uwe Hollenbach

In support of the efforts at IMO in conjunction with the introduction of EEDI regulations, the ITTC (International Towing Tank Conference) has updated its speed and power sea trial procedures outside of its normal sequence of work. The updated procedures submitted to IMO can be found on the ITTC website: <http://itcc.info/news/shortnews/32-seatrials>.

One important amendment will influence the predictions of most model basins worldwide and can be found in the procedure 7.5-04-01-01.1 "Preparation and Conduct

of Speed/Power Trials", chapter 7.5 "Model Test Information". In paragraph 3) it reads; "For all draughts and trims, the same methods, procedures and empirical coefficients shall be used to extrapolate the model scale values to full scale."

At present HSVA determines the correlation allowance for the full scale prediction using an empirical equation derived from former sea trial results. This equation uses the LPP and CB (block coefficient) as parameters and consequently the correlation coefficients used for design and ballast draughts differ, as the block coefficient is not the same for both conditions.

The ITTC now recommends using the same correlation coefficient for all draughts.

We have checked this proposal for a number of vessels where sea trial results and/or feedback from ships in service are available. Based on our analysis we agree to this ITTC proposal, as for most cases it is in line with our own findings and also improves the accuracy of HSVA's predictions. A closer look into this new proposal will be necessary only for full block ships, since a sufficient amount of reliable feedback from bulkers and tankers in loaded condition is not yet available.

Emission Reduction During Port Manoeuvring

✍ by Marco Schneider

Introduction:

When looking at the total emissions of the global ship fleet there is not much to save on the first sight at port manoeuvres. The majority of the vessels operate mainly at seagoing conditions. However the emission reduction during port manoeuvring is an important subject because it mostly takes place in densely populated areas with a strong impact on the health of the local population. The EU-Project TEFLES (Technologies and Scenarios for Low Emissions Shipping, www.tefles.eu) focused on emission reduction of vessels. One technique studied and investigated within the project was the emissions reduction by optimised port manoeuvring.

Description:

The manoeuvring optimisation process requires the interaction of four tools as show in Fig. 1.

The first tool is the HSVA harbour manoeuvring simulator. During harbour manoeuvres dramatic speed changes and even sailing in the opposite direction occur. This requires a four quadrant model that can handle all four combinations of the ship sailing and the propeller thrust directions. Furthermore shallow water effects and environmental conditions like currents and wind forces are important and need to be taken into account.

The required coefficients for the manoeuvring simulator were calculated with the in-house RANS solver *FreSCO+*. Fig. 2 shows an example of the flow around the superstructure for the calculation of the wind-coefficients and Fig. 3 for the hydrodynamic coefficients of the ship hull.

Furthermore a course keeping tool that simulates the job of the captain on a real ship

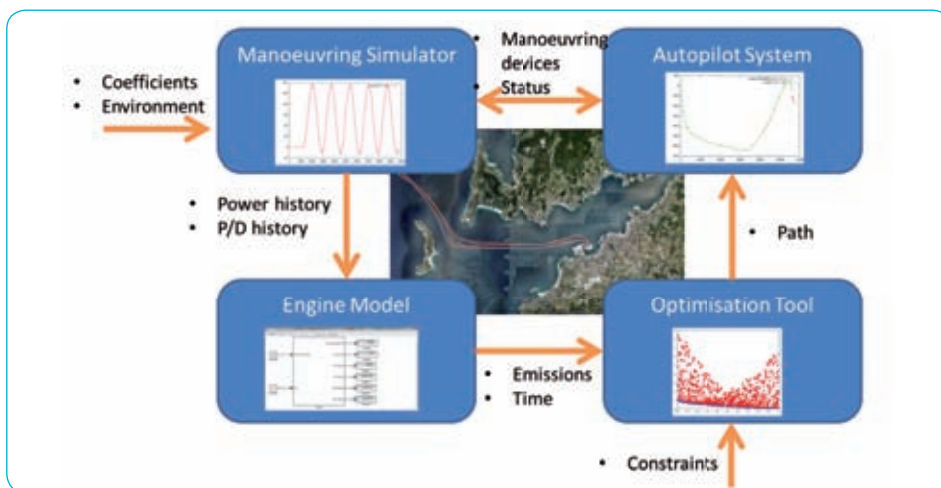


Fig. 1: Flowchart optimisation process

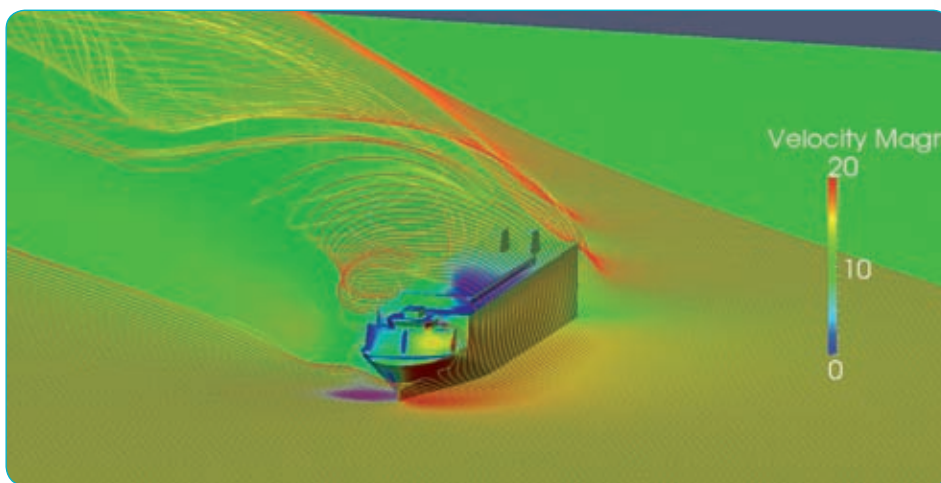


Fig. 2: Streamlines of the flow around the superstructure

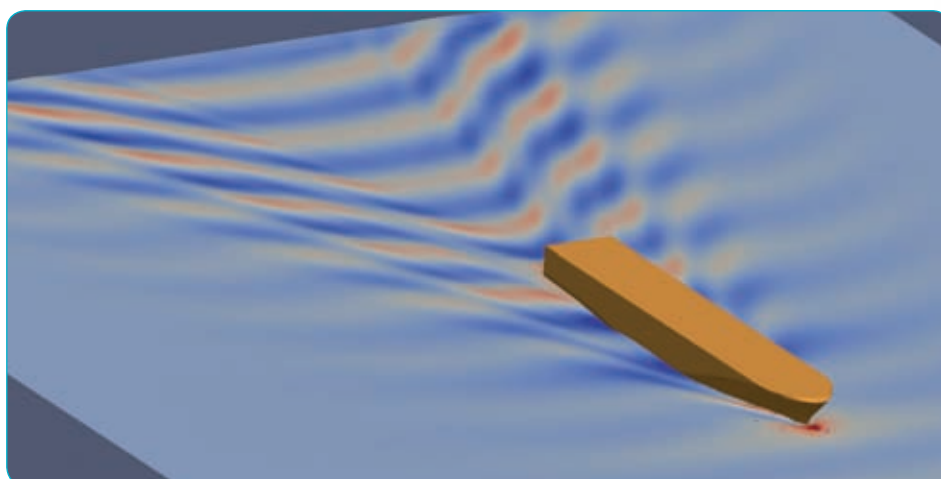


Fig. 3: Wave pattern



Fig. 4: Case ship, car carrier



Fig. 5: Recorded path of the car carrier

is required. The tool is steering the rudder and the engine so that the ship keeps the prescribed path with the prescribed speed. The Engine Module converts the power and P/D history output from the manoeuvring simulator into emissions of CO₂, SO_x, NO_x and PM over time. This tool was provided by the project partner VICUSdt and Newcastle University.

The prescribed combination of tools is sufficient for an investigation of a single prescribed path. However since an optimisation is desired the whole process needs to be run automatically with different paths and speeds. This is done by a genetic multi-objective optimisation. It creates different path and speed profiles dependent on chosen parameters. The two objective functions of the optimisation are the emissions that should be as low as possible and the time that should be as short as possible.

Example:

The whole optimisation process was tested for the port entry of a car carrier into the port of Vigo in Spain. Fig. 4 shows a picture of the vessel and Fig. 5 the recorded path of the vessel during the port entry and exit. The initial population and the Pareto

population of the multi-objective optimisation are shown in Fig. 6. An emission reduction of 18 % is possible with an increase of the manoeuvring time of one minute and 50 seconds. The minimum time for the port manoeuvre is roughly 9.5 minutes. In this case the savings were mostly due to an optimised speed profile of the vessel. The influence of the different paths was relatively small.

Conclusion & Outlook:

The combined tools offer a great possibility of investigating and optimising

the emissions during port manoeuvring. Furthermore a tracking of the emissions for different environmental conditions is a powerful tool for planning and optimisation of harbour facilities.

The research performed in the TEFLES project is partly funded by the European Commission under Grant Agreement 266126 as part of the 7th Framework Surface Transport programme.

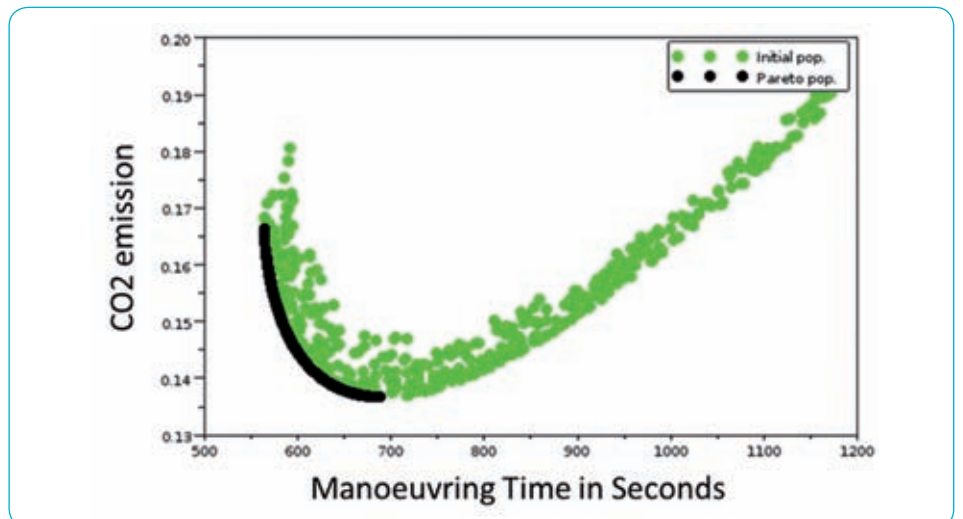


Fig. 6: Optimisation results

Pre-Swirl Stators for Deltamarin: Efficiency in Propulsion Meets Efficient Cooperation

✍ by Heinrich Streckwall and Thomas Lücke

Some years ago Deltamarin came up with the idea to provide bulk carriers with pre-swirl stators to enhance the energy balance for this type of vessel. Deltamarin provided not only this idea but also the general outline and positioning of the fins that should make up such a pre-swirl stator. Within the first stator project it was HSVA's part to perform further adjustments of the stator fins. As a matter of fact, such 'shared work' characterizes all stator-projects ordered since then by Deltamarin.

HSVA considered it a challenge to investigate in detail the working principle and the design target of such a device. In particular it was deduced that the pre-swirl fins needed geometrical adjustments to optimize the pre-swirl benefits for the propeller. It is recorded that the propeller reacts to a suitable pre-swirl with a significant RPM drop. Such drastic performance changes are necessary to arrive at an energy saving system, since the working principle unavoidably requests an enlarged thrust. Comparing model tests performed with and without pre-swirl stators, RPM drops and thrust increases are typical findings. Their final balance enters the propulsion efficiency and identifies the quality of the system.

A demand for efficiency was not only set to the stator's hydrodynamic performance but also to the design strategy. One practical problem met for tests with pre-swirl stators involved is often the limited time left for the completion of the design and the production of the model. It is not unusual that design and making have to be squeezed into a 4 weeks period. The reason for such challenging demands is the close linkage to the design propeller, its final drawings being generally also 'just in time' deliveries.

In this situation the following approach turned out to guarantee a time efficient

process chain. In most of the cooperative stator projects, HSVA base their design work on the calculated wakes at stator and propeller provided by Deltamarin. As part of the design process carried out by HSVA the propeller induced velocities are then added to the wake field taken at the stator plane. With the so completed picture on the flow at the fins the final geometrical adjustment is done in view of the two decisive targets, namely optimum pre-swirl and 'sound' flow along the fins' sections.

Meanwhile stators for 6 projects have been designed like this, which then – except for one design – were fine-tuned and approved by model tests at HSVA. Therefore just a final individual pitching of the fins was necessary during the experiments.

Two of these projects found a full scale installation already - with great success for three reasons:

- A close cooperation with Deltamarin. This was essential to clearly define the freedom as well as the limitation for the optimization procedure.
- Inclusion of propeller considerations in an early lines design stage already. These way large propellers were possible, since propeller induced pressure pulses were considered as an issue from the very beginning.
- Use of powerful numerical and experimental tools from one hand. This allowed efficient combination of both techniques.

The fruitful cooperation with Deltamarin will go on – in near future with stators and propellers optimized as one unit.

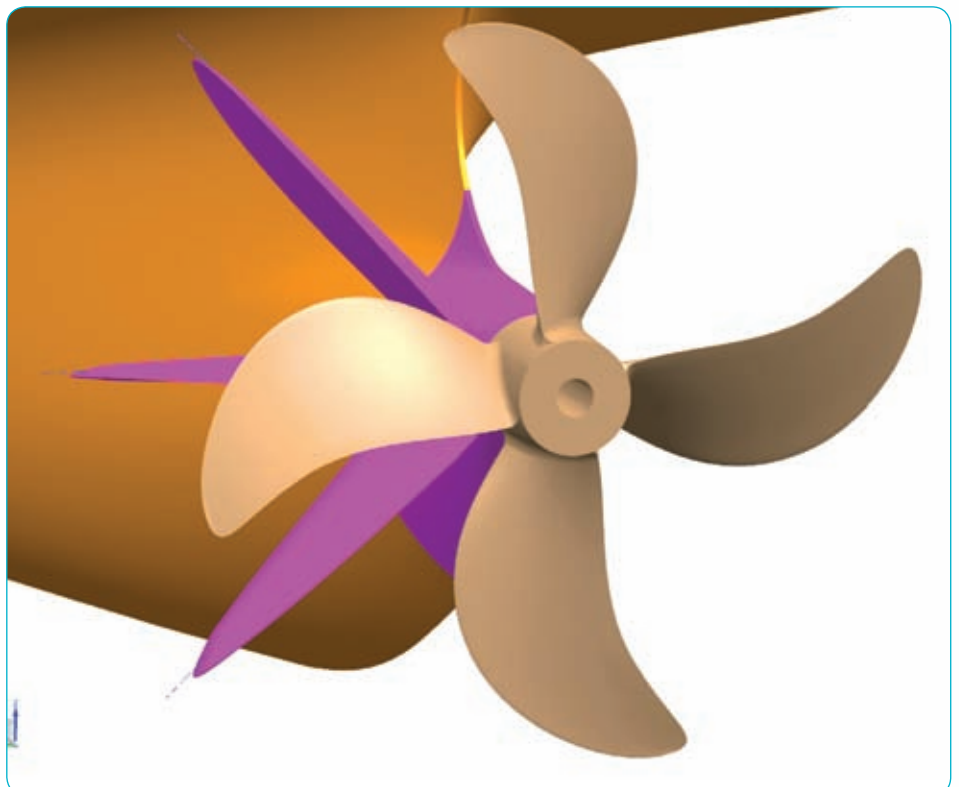


Fig. 1: Propulsion system of the B.Delta37 vessel consists of a cooperatively designed stator and an HSVA propeller design

Member of Staff

The Propellers and Cavitation Department has two new members, Eva Göricke since June 2013 and Julia Müller since October of the same year. They are both project managers and in turn perform cavitation tests in HYKAT and the conventional cavitation tunnels. They are in contact with clients from all over the world. Besides, Julia Müller is involved in open water tests and Eva Göricke evaluates wake measurements.

Eva Göricke studied mechanical engineering with specialization in naval architecture at the University of Duisburg-Essen, Germany. After internships in the Netherlands, she made her

way to Hamburg and did the tests for her diploma thesis in HYKAT.

Julia Müller studied Naval Architecture and Ocean Engineering in Bremen and Sydney for her Bachelor degree and did her Master of Engineering in Kiel. Both her theses were done in cooperation with HSVA.

Eva likes watching classic movies and listening to hard rock music in her spare time if she cannot be on the water sailing or rowing.

Julia enjoys sailing in her Europe dinghy in summer. During winter season she usually



Eva Göricke

Julia Müller

refurbishes her boat. Additionally she likes to read good thick books and to go on bicycle tours.

Cavitation Documentation and HYKAT Control Goes Android

by Christian Johannsen

Many model basins worldwide do documentation of propeller or rudder cavitation phenomena simply by photographs and/or video records. This is easy and cheap indeed, but leaves the customer alone with nice but meaningless pictures. The judgment is missing!

This is why HSVA's customers strongly appreciate our precise cavitation sketches, providing both a detailed description and a reliable judgment at one glance. Many say that those sketches are worthier than all the wording in the report!

Nevertheless, simplicity and quality are here no contradiction anymore, since the time consuming subsequent elaboration of pencil-made live sketches has become redundant. This was possible because sketching nowadays is done directly on an Android

tablet PC. Accurate sketches without post processing are the consequence, being available immediately after the test.

The Android tablet PC also provides another useful technical development. The controls of the whole HYKAT cavitation tunnel are decentralized by linking them to the tablet. All functions are ready for takeaway! Pressure and strobe light control, for example, is possible wherever the observer's view to the cavitating object of interest might be best.

Especially for enduring cavitating tip vortices that never seem to withdraw from the blade tip, the tablet computer gives the opportunity to stay at the observation window, altering the strobe light adjustment and sketching the cavities.

No scientific milestones indeed, but small steps to combine HSVA's well-known quality with increased quickness und effectivity.



**SMM
2014**

**Visit us at SMM, International Maritime Conference & Exhibition,
9th–12th September 2014, Hamburg, Germany.
You can find us in hall no. B4 at our stand no. EG.108.**